

Scalable GWR: A linear-time algorithm for large-scale geographically weighted regression with polynomial kernels

Daisuke Murakami¹, Narumasa Tsutsumida², Takahiro Yoshida³, Tomoki Nakaya⁴, Binbin Lu⁵

¹ Department of Data Science, Institute of Mathematical Statistics, Japan

² Graduate School of Global Environmental Studies, Kyoto University, Japan

³ Center for Global Environmental Studies, National Institute for Environmental Studies, Japan

⁴ Graduate School of Environmental Studies, Tohoku University, Japan

⁵ School of Remote Sensing and Information Engineering, Wuhan University, China

Abstract

While a number of studies have developed fast geographically weighted regression (GWR) algorithms for large samples, none of them achieves the linear-time estimation that is considered requisite for big data analysis in machine learning, geostatistics, and related domains. Against this backdrop, this study proposes a scalable GWR (ScaGWR) for large datasets. The key development is the calibration of the model through a pre-compression of the matrices and vectors whose size depends on the sample size, prior to the execution of leave-one-out cross-validation (LOOCV) that is the heaviest computational step in conventional GWR. This pre-compression allows us to run the proposed GWR extension such that its computation time increases linearly with sample size, whereas conventional GWR algorithms take at most quad-quadratic-order time. With this development, the ScaGWR can be calibrated with more than one million samples without parallelization. Moreover, the ScaGWR estimator can be regarded as an empirical Bayesian estimator that is more stable than the conventional GWR estimator. This study compared the ScaGWR with the conventional GWR in terms of estimation accuracy, predictive accuracy, and computational efficiency using a Monte Carlo simulation. Then, we apply these methods to a residential land analysis in the Tokyo Metropolitan Area. The code for ScaGWR is available in the R package **scgwr**, and is going to be incorporated into another R package, **GWmodel**.

Keywords

Geographically weighted regression, large spatial data, computational complexity, scalability, pre-processing

1. Introduction

Geographically weighted regression (GWR; Brunsdon et al., 1998; Fotheringham, 2002) is a well-known approach for spatially varying coefficient (SVC) modeling. Due to its flexibility and simplicity, GWR has widely been accepted in regional science (e.g., Cahill and Mulligan, 2007; Páez et al., 2008), epidemiology (e.g., Nakaya et al., 2005), and environmental science (e.g., Dong et al., 2018) to investigate spatial heterogeneity in regression coefficients. In spite of its popularity, GWR is limited in application to big spatial data because of the computational complexity of model estimation. Efficient GWR algorithms have been developed by Harris et al. (2010), Tran et al. (2016), and Li et al. (2019) through parallelization. Li et al. (2019) optimized the linear algebra in the GWR algorithm to reduce the required memory storage from $O(N^2)$ to $O(NK)$, where N and K denote the sample size and the number of covariates, respectively. The computational complexity of their proposed fast GWR is $O(K^2N^2\log N)$, meaning that the computational burden grows in a quasi-quadratic manner with N . However, modeling in $O(K^2N^2\log N)$ time is not fast enough as linear-time modeling (i.e., $O(N)$) is expected in the era of big data in geostatistics (see Heaton et al., 2018 for review), machine learning (see Liu et al., 2018 for review), and other fields.

Large spatial data modeling has been studied intensively in geostatistics. Fixed-rank kriging (Cressie and Johannesson, 2008), predictive process modeling (Banerjee et al., 2008), and nearest-neighbor Gaussian process modeling (NNGP; Datta et al., 2016) are instances of linear-time geostatistical approaches. While these approaches aim to model the residual spatial process and interpolate data, Finley et al. (2011) and Datta et al. (2016) extended the predictive process and NNGP modeling to SVC modeling, respectively. However, as noted by Finley et al. (2011), these approaches are still slow for large samples because of the need for the Markov chain Monte Carlo (MCMC) simulation, although the burden is lightened by applying an efficient MCMC procedure (e.g., Finley et al., 2018) or alternatives of MCMC, such as the variational Bayes approach (see Bishop, 2006) and the integrated nested Laplace approximation (Rue et al., 2009). Other computationally efficient SVC modeling approaches include (i) the spatial expansion method (Casetti, 1972); (ii) the bivariate spline-based approach (Mu et al., 2018); and (iii) the Moran eigenvector approach (Murakami et al., 2017; Murakami and Griffith, 2019). (i) and (ii) estimate SVCs by fitting deterministic functions while (iii) estimates them by fitting approximate Gaussian processes that are interpretable in terms of the Moran coefficient (Moran, 1950). All these approaches assume that SVCs are expressed as linear combinations of $L(\ll N)$ spatial basis functions. However, approaches of this kind that use L basis functions are known to suffer from the degeneracy problem (Stein, 2014). That is, they fail to capture small-scale spatial variations when N is large (e.g., $20,000 \leq N$) and the resulting SVCs become overly smooth.

In summary, a practical approach to SVC modeling that fulfills the following requirements is required:

- (i) Linear-time estimation of SVCs;
- (ii) No reliance on MCMC;
- (iii) Not suffering from the degeneracy problem, i.e., small-scale spatial variations should be effectively captured.

With the focus on (iii), GWR, which is a local approach that does not suffer from the degeneracy problem, is an appropriate approach. Thus, we extend GWR to the scalable GWR (ScaGWR) to satisfy all the three requirements above. The remainder of this paper is organized as follows: Section 2 introduces the original GWR and Section 3 develops the ScaGWR. Section 4 compares GWR and ScaGWR through a Monte Carlo simulation, and Section 5 compares them in a residential land price analysis. Finally, Section 6 provides the conclusions of this study.

2. Geographically weighted regression (GWR)

The basic GWR model can be formulated as follows:

$$y_i = \beta_{i,0} + \sum_{k=1}^K x_{i,k} \beta_{i,k} + \varepsilon_i \quad \varepsilon_i \sim N(0, \sigma^2), \quad (1)$$

where $i \in \{1, \dots, N\}$ is an index of sample sites distributed across a geographical space, y_i is the i -th explained variable, $x_{i,k}$ is the k -th covariate, $\beta_{i,0}$ is the intercept parameter, and $\beta_{i,k}$ is the local regression coefficient for the k -th covariate. The regression coefficients $\boldsymbol{\beta}_i = [\beta_{i,0}, \beta_{i,1} \dots \beta_{i,K}]'$ are estimated by a weighted least squares method, where “ $'$ ” denotes the matrix transpose. The estimator is given by

$$\hat{\boldsymbol{\beta}}_i = [\mathbf{X}' \mathbf{G}_i(b) \mathbf{X}]^{-1} \mathbf{X}' \mathbf{G}_i(b) \mathbf{y}, \quad (2)$$

where \mathbf{y} is a vector of the explained variables and \mathbf{X} is a matrix of covariates with a column of 1s for the intercept. $\mathbf{G}_i(b)$ is a diagonal matrix whose j -th element is the geographical weight $g_{i,j}(b)$ for the j -th sample, and can be calculated via a distance-decaying kernel function. For example, the Gaussian kernel in Eq. (3) is a usual choice:

$$g_{i,j}(b) = \exp \left[- \left(\frac{d_{i,j}}{b} \right)^2 \right], \quad (3)$$

where $d_{i,j}$ is the Euclidean distance between s_i and s_j . The distance may be substituted with Minkowski distance (Lu et al., 2016), network distance, travel time, or other non-Euclidean distances (Lu et al., 2014). b is a bandwidth parameter that takes a small (near-zero) value if the regression coefficients have small-scale map patterns and a large value when they have large-scale patterns. As b grows, $\hat{\boldsymbol{\beta}}_i$ asymptotically converges to the ordinally least squares (OLS) estimator: $\hat{\boldsymbol{\beta}}_{OLS} = (\mathbf{X}' \mathbf{X})^{-1} \mathbf{X}' \mathbf{y}$.

The bandwidth b can be optimized by leave-one-out cross-validation (LOOCV) that minimizes the cross-validation (CV) score, which is defined as follows:

$$\text{CV score} = \sum_{i=1}^N \hat{\varepsilon}_i^2, \quad (4)$$

where $\hat{\varepsilon}_i = y_i - \sum_{k=1}^K x_{i,k} \hat{\beta}_{-i,k}$. $\hat{\beta}_{-i,k}$ is estimated using the $N - 1$ samples other than the i -th sample. Specifically, $\hat{\beta}_{-i} = [\hat{\beta}_{-i,1} \cdots \hat{\beta}_{-i,K}]'$ is estimated using Eq. (2), where $\mathbf{G}_i(b)$ is replaced with $\mathbf{G}_{-i}(b)$, which is a diagonal matrix whose elements are summarized as a vector as $\mathbf{g}_{-i}(b) = [g_{1,j}(b), \cdots, g_{i-1,j}(b), 0, g_{i+1,j}(b), \cdots, g_{N,j}(b)]'$.

Figure 1 summarizes the LOOCV procedure in the basic GWR. The grey color shows matrices or vectors whose dimensions depend on sample size. As illustrated in the figure, large matrices must be repeatedly processed to find the optimal b . This is the main reason for why GWR is slow for large N .

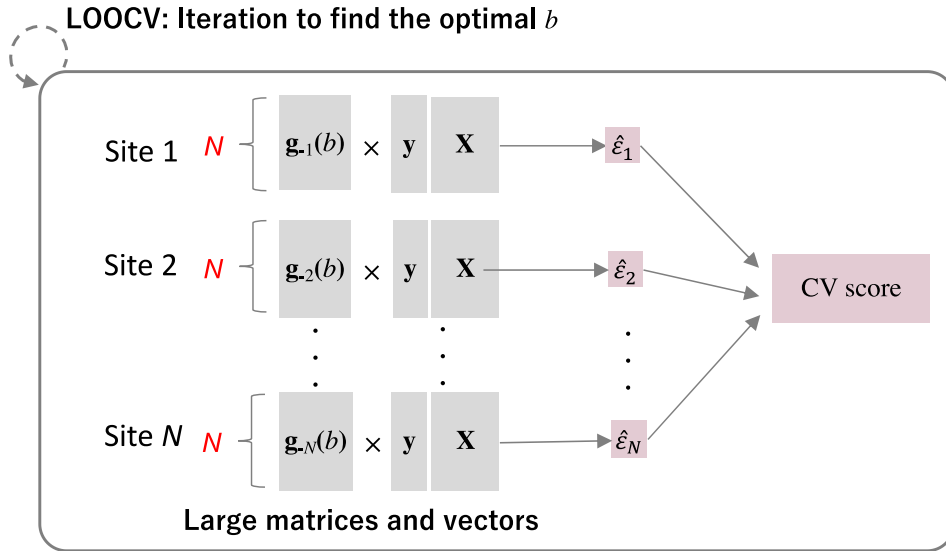


Figure 1: LOOCV routine in the standard GWR. Grey squares represent matrices and vectors whose sizes depend on N , and red squares represent other small elements.

3. Scalable geographically weighted regression (ScaGWR)

Figure 1 suggests that GWR can be accelerated if we let the large matrices/vectors out of the LOOCV iteration. However, the bandwidth parameter b is not separable from $\mathbf{g}_{-i}(b)$ because of the non-linearity of this function; thus, $\mathbf{g}_{-i}(b)$ and other large matrices and vectors must be processed in every LOOCV iteration. We overcome this bottleneck by introducing a linear multiscale kernel that allows us to linearly separate the internal parameters from the kernel function and

pre-process the large matrices and vectors before the iteration. The resulting procedure estimates a regularized GWR model in quasi-linear time. Section 3.1 introduces our ScaGWR model with the multiscale kernel, Section 3.2 explains properties of the SVC estimator, and Section 3.3 shows how to accelerate the LOOCV through the pre-processing.

3.1. Model

The ScaGWR model is identical to the basic GWR model Eq. (1) except for the use of a linear multiscale kernel for fast computation. Section 3.1.1 introduces a linear polynomial kernel that approximates standard kernels and Section 3.1.2 introduces the multiscale kernel, which is an extension of the polynomial kernel.

3.1.1. Linear polynomial kernel

Our kernel must be defined by a linear function to allow the large matrices to get out of the iterative part shown in Figure 1. Although the Taylor or Fourier transformation is available to find a linear approximation of the kernels, our preliminary analysis suggests that their approximation error for the kernels rapidly increases with $d_{i,j}$. Instead, we propose the following polynomial kernel:

$$\tilde{g}_{i,j}^0(\tilde{b}) = \sum_{p=1}^P \tilde{b}^p g_{i,j}(b_0)^{4/2^p}, \quad (5)$$

where $g_{i,j}(b_0)$ is a base kernel with known bandwidth b_0 . We assume that $g_{i,j}(b_0)$ is a non-negative decreasing function with respect to $d_{i,j}$, and is one if $d_{i,j} = 0$. $p \in \{1, \dots, P\}$ represents the degree of the polynomials. This means that the Gaussian kernel (Eq. 3) and the exponential kernel are applicable to the $g_{i,j}(b_0)$ function while kernels with hard thresholds, such as the bi-square and tri-cube kernels, are not. Such a polynomial kernel has often been used for regression problems (e.g., Fan et al., 1995). The means of determining P is unclear. We perform a Monte Carlo simulation to clarify this.

Instead of the known b_0 , we estimate \tilde{b} indicating the spatial scale of the SVCs. For instance, consider a case with three polynomials. In this case, Eq. (5) is $\sum_{p=1}^3 \tilde{b}^p g_{i,j}(b_0)^{4/2^p}$ with known base kernels $\{g_{i,j}(b_0)^2, g_{i,j}(b_0), g_{i,j}(b_0)^{1/2}\}$ and their coefficients $\{\tilde{b}^1, \tilde{b}^2, \tilde{b}^3\}$. $g_{i,j}(b_0)^2 < g_{i,j}(b_0) < g_{i,j}(b_0)^{1/2}$ holds if $d_{i,j} > 0$. In other words, $\{g_{i,j}(b_0)^2, g_{i,j}(b_0), g_{i,j}(b_0)^{1/2}\}$ describes a short-range, moderate-range, and long-range decay of a kernel function. The coefficients $\{\tilde{b}^1, \tilde{b}^2, \tilde{b}^3\}$ assign weights to these kernels. For example, if $\tilde{b} = 0.1$, the weights of the three kernels become $\{0.1, 0.01, 0.001\} \propto \{90.1, 9.0, 0.9\}$. The resulting $\tilde{g}_{i,j}^0(\tilde{b})$ yields a short-range kernel. By contrast, if $\tilde{b} = 10$, the weights become $\{10, 100, 1000\} \approx \{0.9, 9.0, 90.1\}$, implying a long-range kernel. Thus, \tilde{b} replaces the usual bandwidth parameter b . See Figure 2 for another example with $P = 5$.

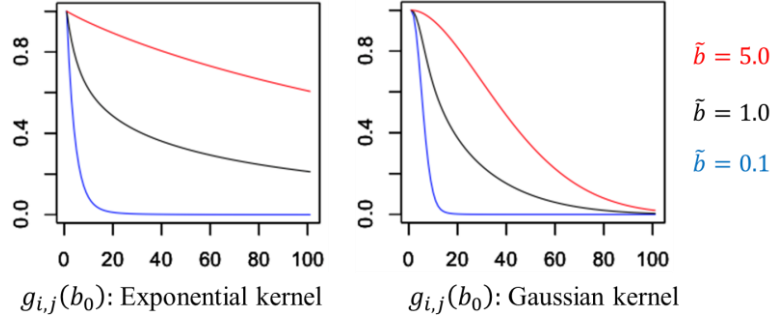


Figure 2: Example of the polynomial kernel with $P = 5$ and $b_0 = 10$

3.1.2. Linear multiscale kernel

The cost of $O(N^2)$ is needed to calculate $\tilde{g}_{i,j}^0(\tilde{b})$ for all $i \in \{1, \dots, N\}$ and $j \in \{1, \dots, N\}$. The use of the polynomial kernel implies failure to achieve the linear-time GWR estimation. To reduce cost, we replace $\tilde{g}_{i,j}^0(\tilde{b})$ with $\tilde{g}_{i,j}(\tilde{b}, \alpha)$, which is specified as

$$\tilde{g}_{i,j}(\tilde{b}, \alpha) = \alpha + \sum_{p=1}^P \tilde{b}^p g_{i,j}^{(Q)}(b_0)^{4/2^p}, \quad (6)$$

where

$$g_{i,j}^{(Q)}(b_0) = \begin{cases} g_{i,j}(b_0) & \text{if } d_{i,j} \leq D_i^{(Q)} \\ 0 & \text{otherwise} \end{cases},$$

α is an unknown parameter, and $D_i^{(Q)}$ is the distance between the i -th site and the Q -th nearest neighbor. $\tilde{g}_{i,j}(\tilde{b}, \alpha)$ weighs the Q -nearest neighbors by [global weight: α] + [local weight: $\sum_{p=1}^P \tilde{b}^p g_{i,j}(b_0)^{4/2^p}$], and the other samples by [global weight: α]. Thus, $\tilde{g}_{i,j}(\tilde{b}, \alpha)$ is a multiscale kernel in which the global and local weights are determined by α and \tilde{b} , respectively. Unlike the polynomial kernel in Eq. (5), the complexity of calculating all $\tilde{g}_{i,j}(\tilde{b}, \alpha)$ s is $O(QN)$, which is trivial as long as Q is small (e.g., 50). Furthermore, as we explain below, the resulting GWR estimator, which is known to suffer from multicollinearity (Wheeler and Tiefelsdorf, 2005), is stabilized if this multiscale specification is used. For these reasons, we prefer the multiscale kernel.

We need to determine the value of the fixed b_0 a priori. If $g_{i,j}(b_0)$ is defined by the Gaussian kernel, we assume $b_0 = D_{med}^{(Q)}/\sqrt{3}$, where $D_{med}^{(Q)}$ is the median of the Q -nearest neighbor distances. This assumption implies $D_{med}^{(Q)} = \sqrt{3}b_0$ = [the effective bandwidth of $g_{i,j}(b_0)$], which is the distance at which 95% of the weight vanishes (see Cressie et al., 1993). That is, the base kernel $g_{i,j}(b_0)$ is assumed to decay gradually across the Q -nearest neighbors, and the speed of decay of the resulting $\tilde{g}_{i,j}(\tilde{b}, \alpha)$ is optimized by estimating \tilde{b} . Because \tilde{b} substitutes b_0 , the ScaGWR estimator is likely to be less sensitive to b_0 , although a sensitivity analysis is an important future topic. In the same manner, we assume $D_{med}^{(Q)} = 3b_0$ for the exponential kernel.

3.2. SVC estimator

The ScaGWR estimator, which is identical to the standard GWR estimator except for the kernel specification, yields

$$\hat{\beta}_i = [\mathbf{X}'\tilde{\mathbf{G}}_i(\tilde{b}, \alpha)\mathbf{X}]^{-1}\mathbf{X}'\tilde{\mathbf{G}}_i(\tilde{b}, \alpha)\mathbf{y}, \quad (7)$$

where $\tilde{\mathbf{G}}_i(\tilde{b}, \alpha)$ is a diagonal matrix whose j -th entry is $\tilde{g}_{i,j}(\tilde{b}, \alpha)$. \tilde{b} and α are estimated by LOOCV minimizing Eq. (4).

The estimator may be rewritten by substituting Eq. (6) into Eq. (7) as

$$\hat{\beta}_i = [\alpha\mathbf{X}'\mathbf{X} + \mathbf{X}'\mathbf{G}_i^{(Q)}(\tilde{b})\mathbf{X}]^{-1} [\alpha\mathbf{X}'\mathbf{y} + \mathbf{X}'\mathbf{G}_i^{(Q)}(\tilde{b})\mathbf{y}], \quad (8)$$

where $\mathbf{G}_i^{(Q)}(\tilde{b})$ is a diagonal matrix whose j -th entry is $\sum_{p=1}^P \tilde{b}^p g_{i,j}^{(Q)}(b_0)^{4/2^p}$. Based on Eq. (8), $\hat{\beta}_i$ can be viewed as an empirical Bayes estimator with prior distribution $\beta^{prior} \sim N(\hat{\beta}_{OLS}, \alpha^{-1}(\mathbf{X}'\mathbf{X})^{-1})$. In other words, ScaGWR stabilizes the GWR estimator by shrinking it toward the OLS estimator, where α determines the degree of shrinkage.

Thus, once the parameters $\{\tilde{b}, \alpha\}$ are given, $\hat{\beta}_i$ is easily estimated. The next section explains our LOOCV procedure to optimize $\{\tilde{b}, \alpha\}$ computationally efficiently.

3.3. LOOCV to optimize parameters $\{\tilde{b}, \alpha\}$

To calculate the CV score in the LOOCV, we need to calculate $\hat{\beta}_{-i}$ for each i repeatedly:

$$\hat{\beta}_{-i} = [\mathbf{X}'\tilde{\mathbf{G}}_{-i}(\tilde{b}, \alpha)\mathbf{X}]^{-1}\mathbf{X}'\tilde{\mathbf{G}}_{-i}(\tilde{b}, \alpha)\mathbf{y}, \quad (9)$$

where $\tilde{\mathbf{G}}_{-i}(\tilde{b}, \alpha)$ is equal to $\tilde{\mathbf{G}}_i(\tilde{b}, \alpha)$ with zero values in the i -th diagonal.

We introduce matrix manipulation to calculate Eq. (9) computationally efficiently. The idea is to pre-process $\mathbf{X}'\tilde{\mathbf{G}}_{-i}(\tilde{b}, \alpha)\mathbf{X}$ and $\mathbf{X}'\tilde{\mathbf{G}}_{-i}(\tilde{b}, \alpha)\mathbf{y}$ that form $\hat{\beta}_{-i}$ before the LOOCV. The (k, k') -th element of $\mathbf{X}'\tilde{\mathbf{G}}_{-i}(\tilde{b}, \alpha)\mathbf{X}$ is analytically obtained as

$$\sum_{j \neq i} \tilde{g}_{i,j}(\tilde{b}, \alpha) x_{j,k} x_{j,k'} \quad (10)$$

By substituting Eq. (6) into Eq. (10), it is further expanded as

$$\begin{aligned} \sum_{j \neq i} \sum_{p=1}^P \left(\alpha + \tilde{b}^p g_{i,j}^{(Q)}(b_0)^{4/2^p} \right) x_{j,k} x_{j,k'} &= \alpha \sum_{j \neq i} x_{j,k} x_{j,k'} + \sum_{p=1}^P \tilde{b}^p \sum_{j \neq i} g_{i,j}^{(Q)}(b_0)^{4/2^p} x_{j,k} x_{j,k'} \\ &= \alpha m_{-i,k,k'}^{(0)} + \sum_{p=1}^P \tilde{b}^p m_{-i,k,k'}^{(p)} \end{aligned} \quad (11)$$

where $m_{-i,k,k'}^{(0)} = \sum_{j \neq i} x_{j,k} x_{j,k'}$ and $m_{-i,k,k'}^{(p)} = \sum_{j \neq i} g_{i,j}^{(Q)}(b_0)^{4/2^p} x_{j,k} x_{j,k'}$. Similarly, the k -th element of $\mathbf{X}'\mathbf{G}_i(b)\mathbf{y}$ is given by

$$\sum_{j \neq i} \tilde{g}_{i,j}(\tilde{b}) x_{j,k} y_j = \alpha m_{-i,k,y}^{(0)} + \sum_{p=1}^P \tilde{b}^p m_{-i,k,y}^{(p)} \quad (12)$$

where $m_{-i,k,y}^{(0)} = \sum_{j \neq i} x_{j,k} y_j$ and $m_{-i,k,y}^{(p)} = \sum_{j \neq i} g_{i,j}(b_0)^{4/2^p} x_{j,k} y_j$. By substituting Eqs. (11) and (12) into Eq. (9), $\hat{\beta}_{-i}$ yields:

$$\hat{\beta}_{-i} = \begin{bmatrix} \alpha m_{-i,k,y}^{(0)} + \sum_{p=1}^P \tilde{b}^p m_{-i,1,1}^{(p)} & \cdots & \alpha m_{-i,k,y}^{(0)} + \sum_{p=1}^P \tilde{b}^p m_{-i,1,K}^{(p)} \\ \vdots & \ddots & \vdots \\ \alpha m_{-i,k,y}^{(0)} + \sum_{p=1}^P \tilde{b}^p m_{-i,K,1}^{(p)} & \cdots & \alpha m_{-i,k,y}^{(0)} + \sum_{p=1}^P \tilde{b}^p m_{-i,K,K}^{(p)} \end{bmatrix}^{-1} \begin{bmatrix} \alpha m_{-i,1,y}^{(0)} + \sum_{p=1}^P \tilde{b}^p m_{-i,1,y}^{(p)} \\ \vdots \\ \alpha m_{-i,K,y}^{(0)} + \sum_{p=1}^P \tilde{b}^p m_{-i,K,y}^{(p)} \end{bmatrix}, \quad (13)$$

which has the following matrix expression:

$$\hat{\beta}_{-i} = \left[\alpha \mathbf{M}_{-i}^{(0)} + \sum_{p=1}^P \tilde{b}^p \mathbf{M}_{-i}^{(p)} \right]^{-1} \left[\alpha \mathbf{m}_{-i}^{(0)} + \sum_{p=1}^P \tilde{b}^p \mathbf{m}_{-i}^{(p)} \right]. \quad (14)$$

where $\mathbf{M}_{-i}^{(0)}$ and $\mathbf{M}_{-i}^{(p)}$ are $K \times K$ matrices whose (k, k') -th elements are $m_{-i,k,k'}^{(0)}$ and $m_{-i,k,k'}^{(p)}$, respectively, whereas $\mathbf{m}_{-i}^{(0)}$ and $\mathbf{m}_{-i}^{(p)}$ are $K \times 1$ vectors whose k -th elements are $m_{-i,k,y}^{(0)}$ and $m_{-i,k,y}^{(p)}$, respectively.

Importantly, because $\{\mathbf{M}_{-i}^{(0)}, \mathbf{M}_{-i}^{(p)}, \mathbf{m}_{-i}^{(0)}, \mathbf{m}_{-i}^{(p)}\}$ do not include any parameter, they can be calculated before the LOOCV. Given these elements, the computational complexity of calculating $\hat{\beta}_{-i}$ is only $O(K^3)$. Thus, the cost of calculating all $i \in \{1, \dots, N\}$ is $O(K^3 N)$. Thus, if the golden section algorithm, whose expected number of iterations is $O(\log(N))$, is used, the complexity of the LOOCV is $O(K^3 N \log(N))$, which is a quasi-linear computational complexity with respect to N . The complexity is considerably smaller than that of current GWR algorithms whose complexity is $O(K^3 N^2 \log(N))$ at best.

In summary, suppose $\mathbf{M}_{-i} \in \{\mathbf{M}_{-i}^{(0)}, \mathbf{M}_{-i}^{(p)}, \mathbf{m}_{-i}^{(0)}, \mathbf{m}_{-i}^{(p)}\}$. Then, the ScaGWR modeling procedure is summarized as follows:

- (i) Pre-processing: \mathbf{M}_{-i} is calculated for each i .
- (ii) LOOCV : $\{\tilde{b}, \alpha\}$ are optimized by the LOOCV in which the CV score is calculated by substituting the inner products in \mathbf{M}_{-i} into Eq. (14). As explained above, the complexity of this step is only $O(K^3 N \log(N))$ (see Figure 3).
- (iii) Estimation : $\hat{\beta}_i$ is estimated by substituting the estimated $\{\tilde{b}, \alpha\}$ into Eq. (15), which is equal to Eq. (8):

$$\hat{\beta}_i = \left[\alpha \mathbf{M}^{(0)} + \sum_{p=1}^P \tilde{b}^p \mathbf{M}_i^{(p)} \right]^{-1} \left[\alpha \mathbf{m}^{(0)} + \sum_{p=1}^P \tilde{b}^p \mathbf{m}_i^{(p)} \right]. \quad (15)$$

where the (k, k') -th elements of the matrices $\mathbf{M}^{(0)}$ and $\mathbf{M}_i^{(p)}$ are given by $\sum_j x_{j,k} x_{j,k'}$ and $\sum_j g_{i,j}(b_0)^{4/2^p} x_{j,k} x_{j,k'}$, respectively, and the k -th elements of the vectors $\mathbf{m}^{(0)}$ and $\mathbf{m}_i^{(p)}$ by $\sum_j x_{j,k} y_j$ and $\sum_j g_{i,j}(b_0)^{4/2^p} x_{j,k} y_j$, respectively.

Note that the equality of Eqs. (8) and (15) means that $\mathbf{M}^{(0)} = \mathbf{X}'\mathbf{X}$, $\sum_{p=1}^P \tilde{b}^p \mathbf{M}_i^{(p)} = \mathbf{X}'\mathbf{G}_i^{(Q)}(\tilde{\mathbf{b}})\mathbf{X}$, $\mathbf{m}^{(0)} = \mathbf{X}'\mathbf{y}$, and $\sum_{p=1}^P \tilde{b}^p \mathbf{m}_i^{(p)} = \mathbf{X}'\mathbf{G}_i^{(Q)}(\tilde{\mathbf{b}})\mathbf{y}$.

It is possible to calculate the standard errors of the coefficients, degrees of freedom, corrected Akaike Information Criterion (AICc), and other statistics to infer the modeling results in linear time (see Appendix 1). The LOOCV in step (ii) can be substituted with an AICc minimization-based optimization that is widely used for bandwidth selection (e.g., Nakaya et al., 2005). See Appendix 1 for further details.

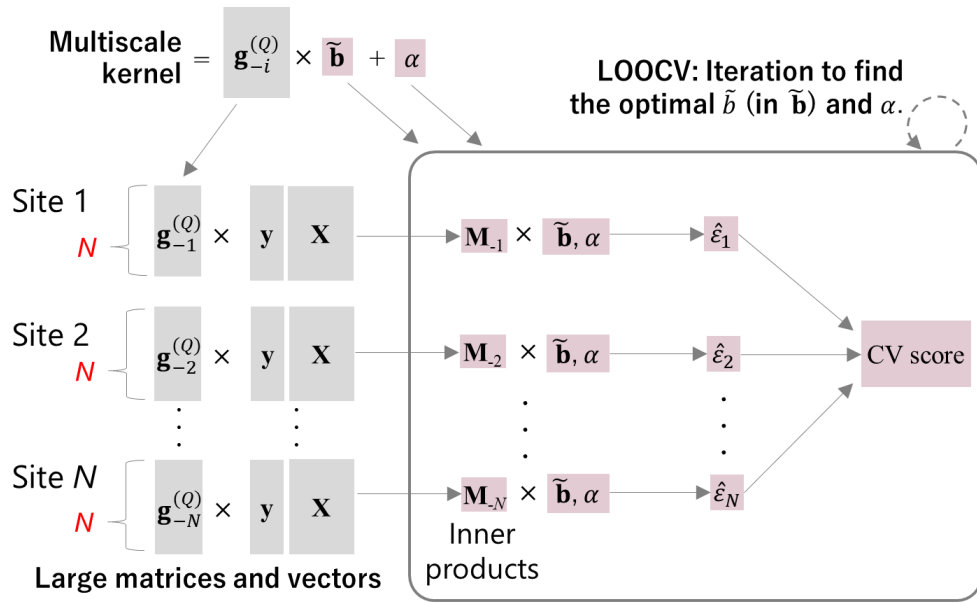


Figure 3: LOOCV routine in the ScaGWR. Grey squares represent large matrices and vectors whose sizes depend on N , and the red squares represent the other small elements. Our multiscale kernel $\mathbf{g}_{-i}^{(Q)}\tilde{\mathbf{b}} + \alpha\mathbf{1}$ includes parameters α and $\tilde{\mathbf{b}}$ optimized by the LOOCV. $\tilde{\mathbf{g}}_{-i}^{(Q)}$ is a matrix of P polynomials and $\tilde{\mathbf{b}} = [\tilde{b}^1, \dots, \tilde{b}^P]'$ is a vector of their coefficients.

4. Monte Carlo simulation experiment

4.1. Outline

This section compares the estimation accuracies and computation times of GWR and ScaGWR through a Monte Carlo simulation. For ScaGWR, we considered the following cases: the number of neighbors $Q \in \{50, 100, 200\}$ and the number of polynomials $P \in \{1, 2, 3, 4, 6\}$. The Gaussian kernel was used in GWR while the same kernel was employed as the base kernel $g_{i,j}(b_0)$ in ScaGWR. We used a Mac Pro (3.5 GHz, 6-Core Intel Xeon E5 processor with 64 GB memory) for

the computation, R (version 3.6.2; <https://cran.r-project.org/>) for model estimation, and the R package GWmodel (version 2.0-5; see Lu et al., 2014b; Gollini et al., 2015), for GWR calibration. The R code of ScaGWR was written using only routines in R. In other words, we did not use Rcpp or other packages to run functions on C++ or other faster environments. Moreover, we did not parallelize the computation.

The X and Y coordinates of the sample sites were randomly determined using two standard normal distributions, $N(\mathbf{0}, \mathbf{I})$. In each site, true data were generated from Eq. (16):

$$\begin{aligned} \mathbf{y} &= \boldsymbol{\beta}_0 + \mathbf{x}_1 \cdot \boldsymbol{\beta}_1 + \mathbf{x}_2 \cdot \boldsymbol{\beta}_2 + \boldsymbol{\varepsilon} \quad \boldsymbol{\varepsilon} \sim N(\mathbf{0}, \sigma^2 \mathbf{I}), \\ \boldsymbol{\beta}_0 &\sim N(\mathbf{1}, 0.5^2 \hat{\mathbf{G}}), \quad \boldsymbol{\beta}_1 \sim N(\mathbf{1}, 2^2 \hat{\mathbf{G}}), \quad \boldsymbol{\beta}_2 \sim N(\mathbf{1}, 0.5^2 \hat{\mathbf{G}}), \end{aligned} \quad (16)$$

where “ \cdot ” is the element-wise product. $\boldsymbol{\beta}_1$, whose variance is 2^2 , explains more spatial variations than $\boldsymbol{\beta}_0$ and $\boldsymbol{\beta}_2$, whose variance is 0.5^2 . Later, we refer to $\boldsymbol{\beta}_1$ as strong SVC and $\{\boldsymbol{\beta}_0, \boldsymbol{\beta}_2\}$ as weak SVCs. $\hat{\mathbf{G}}$ is a Nystrom approximation (see Grineas and Mahoney, 2005) of a kernel matrix \mathbf{G} , which in itself is difficult to handle when N is large. The (i, j) -th element of \mathbf{G} is $g(d_{i,j}) = \exp\left(-\frac{d_{i,j}^2}{b^2}\right)$. Following Dray et al. (2006) and Murakami et al. (2017), b is given by the maximum distance in the minimum spanning tree connecting samples. ScaGWR was estimated while varying $N \in \{500, 1000, 3000, 5000, 7000, 10000, 20000, 40000, 60000, 80000\}$ while GWR was estimated in the six cases with $N \leq 10000$. For each N , the estimation was iterated 200 times.

To calculate the SVC estimation error, we used the root mean-squared error (RMSE):

$$RMSE[\hat{\beta}_{i,k}] = \sqrt{\frac{1}{200N} \sum_{iter=1}^{200} \sum_{i=1}^N (\hat{\beta}_{i,k}^{iter} - \beta_{i,k})^2}, \quad (17)$$

where $\hat{\beta}_{i,k}^{iter}$ is the coefficient estimated in the $iter$ -th iteration.

4.2. Results

Figures 4 and 5 summarize the RMSEs for small to moderate samples ($N \leq 10,000$) and larger samples ($80,000 \leq N$), respectively. They show that the strong and weak SVCs had different tendencies.

When $N < 10,000$, ScaGWR accurately estimated the strong SVC ($\boldsymbol{\beta}_1$) if P and Q were small. A smaller P reduced the number of polynomials while a smaller Q implied less dependence on local weights. Thus, the accurateness is attributable to the parsimony of this specification. Because GWR easily suffers from local collinearity, the result indicating the accuracy of the parsimonious specification is reasonable. As N increased, the accuracy of the ScaGWR estimates for the strong SVC improved and, roughly when $10,000 \leq N$, the RMSE values were similar across values of P and Q .

Weak SVCs ($\boldsymbol{\beta}_0, \boldsymbol{\beta}_2$) indicate better accuracy when P and Q are large. This was opposite to

the tendency in case of the strong SVC. This suggests that more parameters are needed to identify weak spatially varying signals. Based on Figure 5, Q determined the scalability of the estimation accuracy. Specifically, $Q = 50, 100$, and 200 yielded slower, moderate, and faster decays of RMSE values as N increased. A large Q is desirable to estimate weak SVCs accurately from large samples. Still, $Q = 100$ achieved reasonable accuracy across cases (see Figure 5).

Overall, accuracy of the ScaGWR estimates tended to outperform the classical GWR. This might be because ScaGWR estimates both local and global structure using \tilde{b} and α , whereas GWR considers only the former. Among the ScaGWR specifications, we prefer $P = 4$ and $Q = 100$ because it achieves reasonable estimation accuracy regardless of whether N is small or large. Figure 6 plots the true and estimated SVCs in first iterations with $N \in \{500, 5,000, 80,000\}$. This figure confirms that ScaGWR with $P = 4$ and $Q = 100$ accurately estimates the SVCs. ScaGWR successfully captures small-scale variations even if $N = 80,000$ whereas GWR is not feasible because of the large samples. It is important to note that other fast approaches, which specify each SVC using linear combinations of L spatial bases, typically fail to capture such small variations due to the degeneracy problem (see Section 1).

Figure 7 compares the CV score, which is a measure of out-of-sample prediction accuracy. ScaGWR achieved higher prediction accuracy than GWR in many cases, especially on large samples. ScaGWR is thus a faster and more accurate alternative to the standard GWR for spatial prediction.

Finally, Figure 8 summarizes the average computation (CP) time. The CP time of the standard GWR rapidly increased with N . It took 2022.3 seconds when $N = 10,000$. By contrast, the CP time of ScaGWR increased only linearly with N . On average, ScaGWR with $Q = 100$ and $P = 4$ took 47.7 seconds for execution when $N = 10,000$ and 338.3 seconds when $N = 80,000$. Even if $N = 1,000,000$, the ScaGWR took only 5,172 seconds (86.2 minutes) on average in five trials without parallelization.

In summary, the ScaGWR with $Q = 100$ and $P = 4$ is more accurate and faster than the basic GWR.

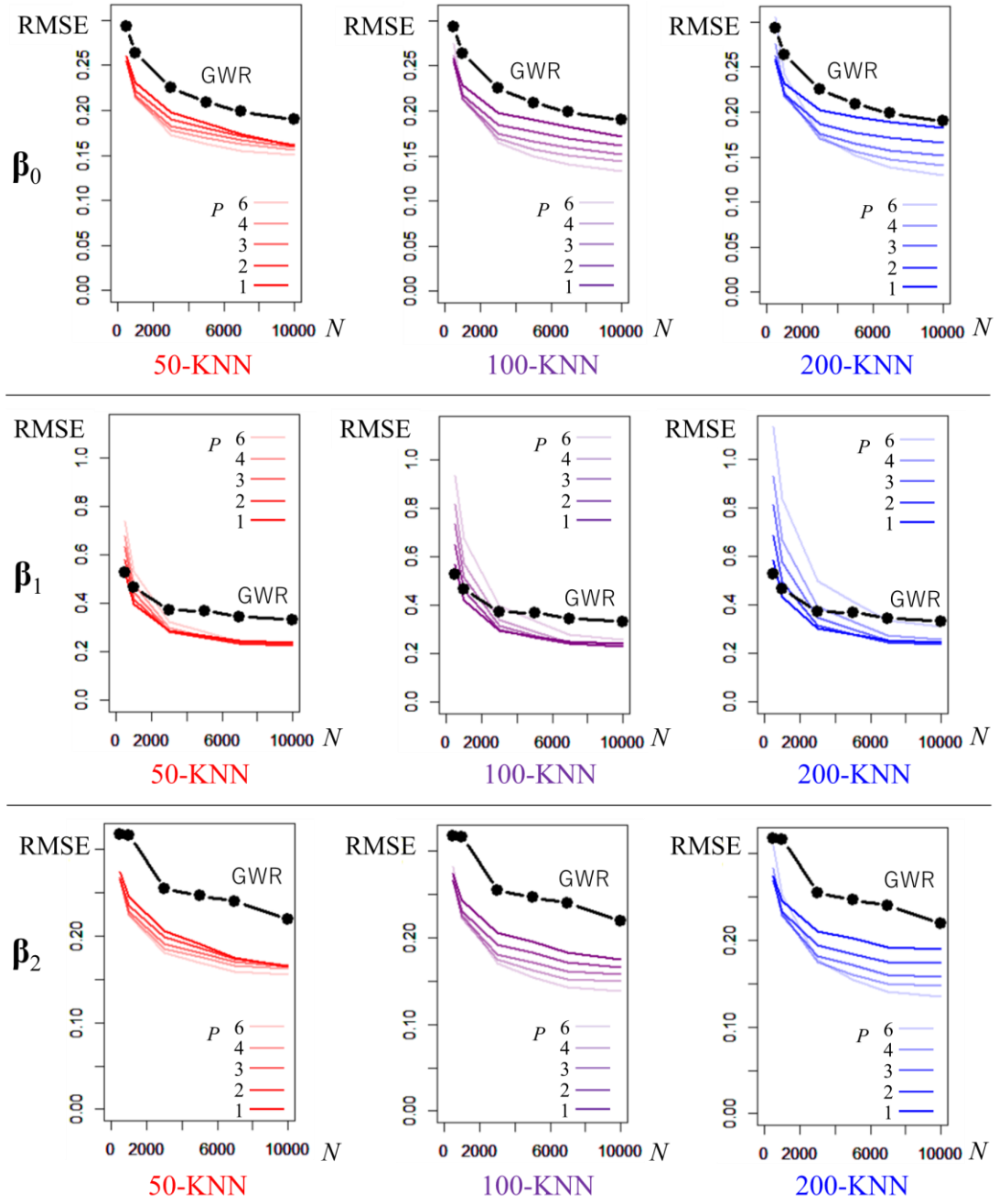


Figure 4: RMSE of SVCs ($10,000 \leq N$)

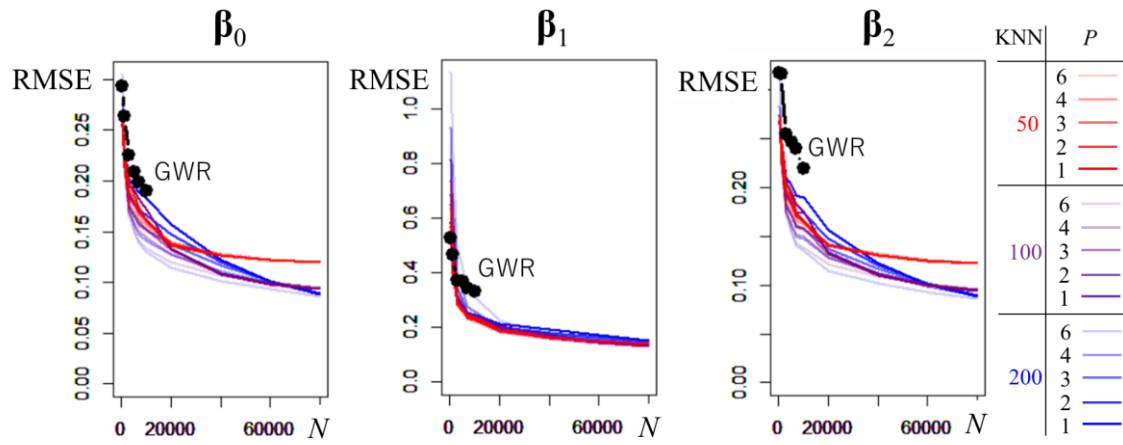


Figure 5: RMSE of SVCs ($80,000 \leq N$)

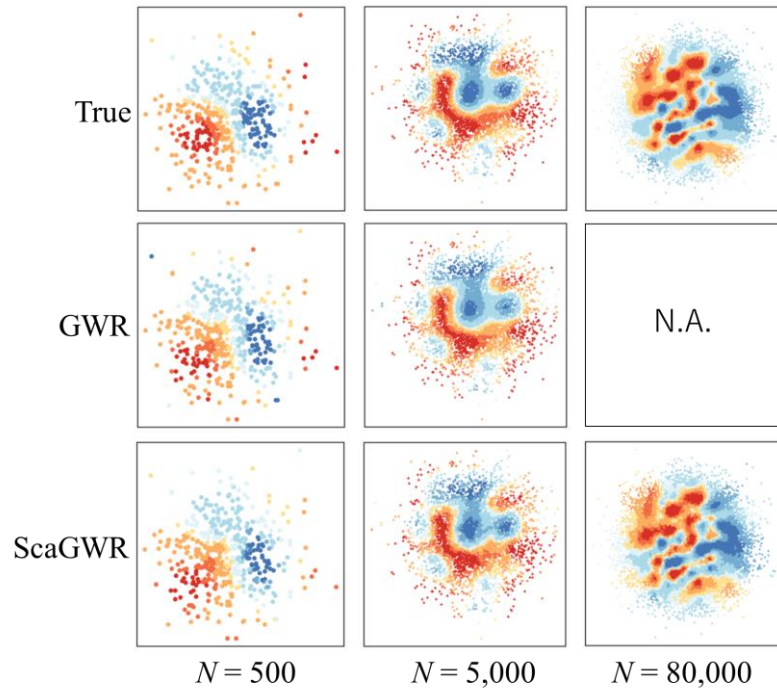


Figure 6: True and estimated SVCs (β_1) in each first iteration. $P=4$ and $Q=100$ was assumed for ScaGWR.

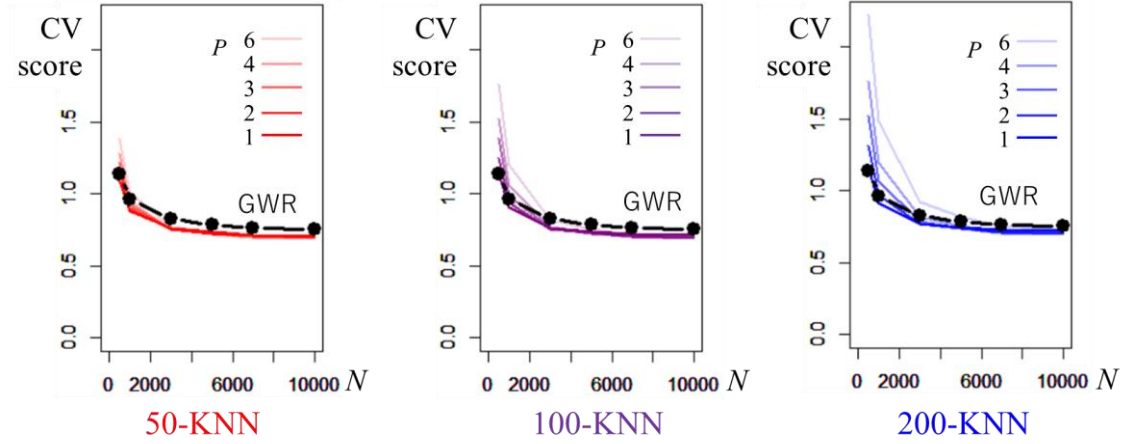


Figure 7: CV scores of GWR (black line) and ScaGWR (colored lines)

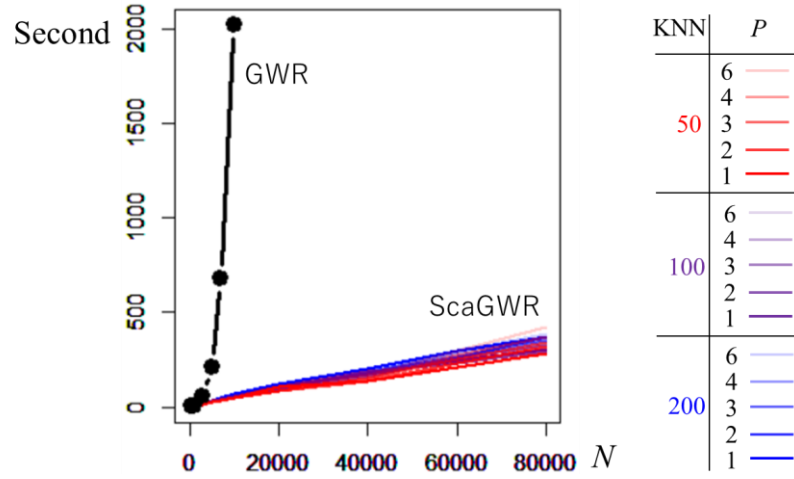


Figure 8: Computation times of GWR and ScaGWR calibrations

5. Application to land price analysis

5.1. Outline

This section applies GWR and ScaGWR with $Q = 100$ and $P = 4$ to a land price analysis in 2015 in the Tokyo Metropolitan Area. The Gaussian kernel was again used, and the package GWmodel was used for the GWR calibration. The explained variables were logged officially assessed residential land prices (JPN/m²; Figure 9). The sample size was 6,363. The covariates were as follows: the share of agricultural area in 1 km grids [Agri]; share of forest in grids [Forest]; Euclidean distance to the nearest railway station (km) [Rail]; and, the Euclidean distance to the nearest bus stop (km) [Bus]. SVCs for these covariates are denoted by $\{\beta_{Agri}, \beta_{Forest}, \beta_{Rail}, \beta_{Bus}\}$. All data were available from the National Land Numerical Information download service, Japan

(<http://nlftp.mlit.go.jp/ksj-e/index.html>).

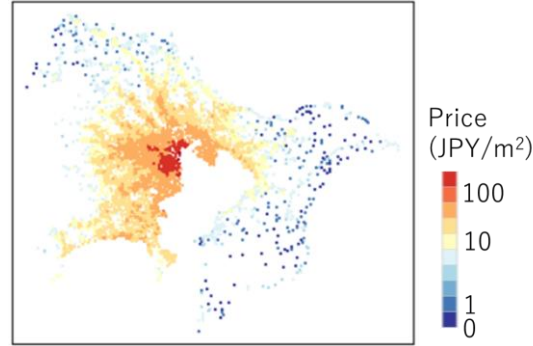


Figure 9: Residential land price (2015)

5.2. Result

Figure 10 summarizes the estimated SVCs. For each panel, darker red represents a larger negative value while darker blue represents a larger positive value. This figure suggests that the GWR and ScaGWR estimates were similar.

For both models, β_{Agri} and β_{Forest} indicate negative values suggesting the preference for convenient urban areas over green areas. β_{Agri} had a negative impact in the center of Tokyo as well, as an increase in agricultural area was not preferable in terms of residential land price. By contrast, β_{Forest} had a strong positive impact near the center. This shows greenery increased the attractiveness of neighborhoods near the center but not in suburban neighborhoods.

β_{Rail} had a negative impact across the study area. The coefficients were especially large near the center. This result confirmed the popularity of nearby stations. β_{Bus} also had a strong negative impact in the Tokyo prefecture. The bus network managed by the prefecture was densely stretched across Tokyo. The result shows that the Tokyo bus network successfully increased the attractiveness of neighborhoods. Such a positive impact is not conceivable in major cities outside Tokyo, including Saitama and Chiba. Still, a negative β_{Bus} , implying higher values of nearby areas with bus stops, was estimated in most other suburban areas.

Thus, this section confirms that ScaGWR estimates interpretable coefficients just like the standard GWR.

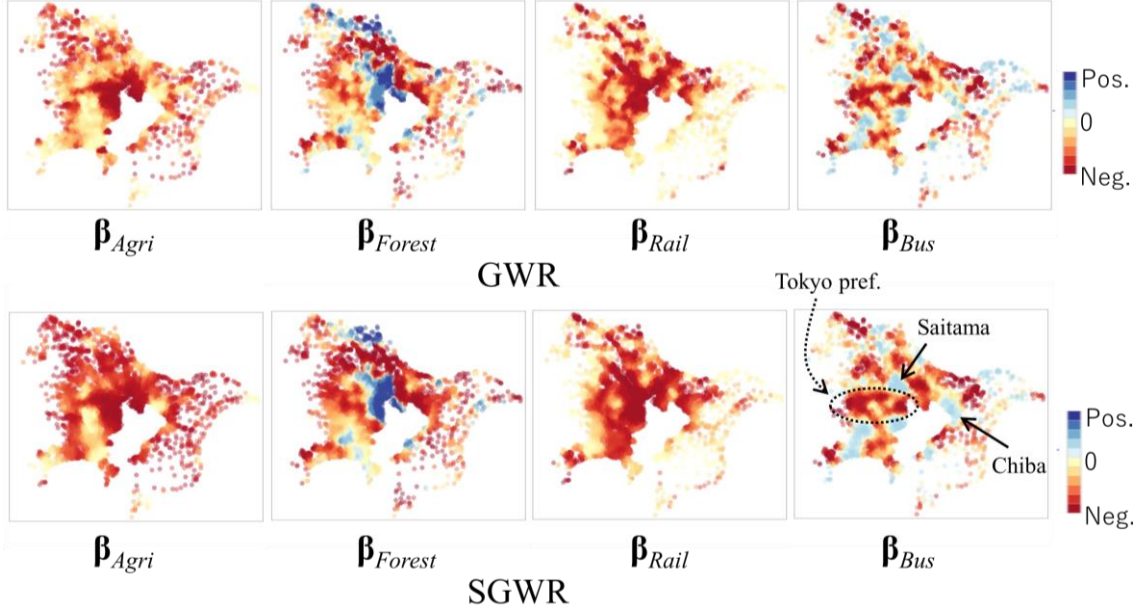


Figure 10: Estimation results

6. Concluding remarks

This study proposed the ScaGWR for large-scale SVC modeling. Unlike current GWR algorithms whose computational complexity is at best quasi-quadratic with respect to N , ScaGWR achieves a quasi-linear computational complexity as illustrated in Figure 8. This property allows us to estimate SVCs from millions of samples even without parallelization. Of course, the parallelization of ScaGWR is an interesting topic for even larger samples in future research.

As reviewed in Section 1, many of efficient approaches for SVC modeling assume that each SVC obeys a linear combination of L spatial basis functions, and suffer from the degeneracy problem; i.e., estimated SVCs tend to have over-smoothed map patterns (Stein, 2014). By contrast, ScaGWR, which performs local estimation, does not suffer from this problem. Figure 6 confirms that ScaGWR successfully captures local variations in SVCs. Thus, it satisfies all the requirements listed in Section 1, including (i) a linear-time computational burden; (ii) no reliance on MCMC; and (iii) no suffering the degeneracy problem

A drawback of GWR is its tendency to suffer from local multicollinearity. Even if a regularization parameter is imposed, GWR, which considers only samples within a kernel window, might be unstable if samples within the window are few. By contrast, ScaGWR implicitly imposes $\beta^{prior} \sim N(\hat{\beta}_{OLS}, \alpha^{-1}(\mathbf{X}'\mathbf{X})^{-1})$ as a prior (see Section 3.3). Therefore, even if the kernel window is small (i.e., \tilde{b} is small), the estimator, which is shrunk to the OLS estimator, is likely to be stable. The robustness of ScaGWR needs to be studied in future work.

Extending ScaGWR is an interesting subject for future research. Its computational

efficiency might be preserved even if it is extended to multiscale GWR (Fotheringham et al., 2017; Lu et al. 2019; Oshan et al. 2019), like GWR with parameter-specific distance matrices (Lu et al., 2017; 2018), GWR with flexible bandwidth (Yang, 2014; Murakami et al., 2019), and conditional GWR (Leong and Yue 2017). Furthermore, ScaGWR might be important in combining GWR with a global model (see, Geniaux and Martinetti, 2018; Harris, 2019). The ScaGWR model can be considered an integration of the GWR model and a global linear regression model. The linear regression is potentially substituted with a mixed effects model, additive model, temporal model, and so on. Such multi-model integration is an interesting development toward the fast, stable, and flexible reformulation of GWR.

ScaGWR was implemented in the R package **scgwr** (<https://cran.r-project.org/web/packages/scgwr/>). We will also consider implementing ScaGWR in the **GWmodel** package embedded into C++ code via the Rcpp package (Eddelbuettel, 2013).

Appendix 1: Diagnostic statistics for ScaGWR

Because the ScaGWR model is equivalent to the basic GWR with the multiscale kernel, its diagnostics are the same as well. The effective sample size of the ScaGWR model, which is required to evaluate the standard errors in the coefficient, is defined as in the GWR as

$$N^* = N - 2tr[\mathbf{S}] + tr[\mathbf{S}'\mathbf{S}], \quad (\text{A1})$$

where \mathbf{S} is the design matrix of the ScaGWR model, specified as

$$\mathbf{S} = \begin{bmatrix} s_{1,1} & s_{1,2} & \cdots & s_{1,N} \\ s_{2,1} & s_{2,2} & \cdots & s_{2,N} \\ \vdots & \vdots & \ddots & \vdots \\ s_{N,1} & s_{N,2} & \cdots & s_{N,N} \end{bmatrix} = \begin{bmatrix} \mathbf{s}'_1 \\ \mathbf{s}'_2 \\ \vdots \\ \mathbf{s}'_N \end{bmatrix} = \begin{bmatrix} \mathbf{x}_1(\mathbf{X}'\tilde{\mathbf{G}}_1(\tilde{b}, \alpha)\mathbf{X})^{-1}\mathbf{X}'\tilde{\mathbf{G}}_1(\tilde{b}, \alpha) \\ \mathbf{x}_2(\mathbf{X}'\tilde{\mathbf{G}}_2(\tilde{b}, \alpha)\mathbf{X})^{-1}\mathbf{X}'\tilde{\mathbf{G}}_2(\tilde{b}, \alpha) \\ \vdots \\ \mathbf{x}_N(\mathbf{X}'\tilde{\mathbf{G}}_N(\tilde{b}, \alpha)\mathbf{X})^{-1}\mathbf{X}'\tilde{\mathbf{G}}_N(\tilde{b}, \alpha) \end{bmatrix}, \quad (\text{A2})$$

where \mathbf{S} is a large matrix ($N \times N$) that cannot be stored for large values of N . However, $tr[\mathbf{S}]$ can be calculated without explicitly processing \mathbf{S} as follows:

$$\begin{aligned} tr[\mathbf{S}] &= \sum_i s_{i,i} = \sum_i \mathbf{x}_i(\mathbf{X}'\tilde{\mathbf{G}}_i(\tilde{b}, \alpha)\mathbf{X})^{-1}\mathbf{x}'_i\tilde{g}_{i,i}(\tilde{b}, \alpha) \\ &= \sum_i \mathbf{x}_i \left[\alpha\mathbf{M}^{(0)} + \sum_{p=1}^P \tilde{b}^p \mathbf{M}_i^{(p)} \right]^{-1} \mathbf{x}'_i \tilde{g}_{i,i}(\tilde{b}, \alpha), \end{aligned} \quad (\text{A3})$$

where $\left[\alpha\mathbf{M}^{(0)} + \sum_{p=1}^P \tilde{b}^p \mathbf{M}_i^{(p)} \right]^{-1}$ is a small matrix ($K \times K$) that has already been calculated when estimating $\hat{\beta}_i$. Thus, $tr[\mathbf{S}]$ is calculated computationally efficiently using Eq. (A3).

Likewise, $tr[\mathbf{S}'\mathbf{S}]$ can be calculated without processing the large matrix $\mathbf{S}'\mathbf{S}$ using

$tr[\mathbf{S}'\mathbf{S}] = \sum_i \sum_j s_{i,j}^2$ as follows:

$$\begin{aligned}
tr[\mathbf{S}'\mathbf{S}] &= \sum_i \sum_j s_{i,j}^2 = \sum_i \mathbf{s}'_i \mathbf{s}_i \\
&= \sum_i \mathbf{x}_i \left[\alpha \mathbf{M}^{(0)} + \sum_{p=1}^P \tilde{b}^p \mathbf{M}_i^{(p)} \right]^{-1} \mathbf{X}' \tilde{\mathbf{G}}_i(\tilde{b}, \alpha)^2 \mathbf{X} \left[\alpha \mathbf{M}^{(0)} + \sum_{p=1}^P \tilde{b}^p \mathbf{M}_i^{(p)} \right]^{-1} \mathbf{x}'_i \\
&= \sum_i \mathbf{x}_i \left[\alpha \mathbf{M}^{(0)} + \sum_{p=1}^P \tilde{b}^p \mathbf{M}_i^{(p)} \right]^{-1} \mathbf{X}' (\alpha \mathbf{I} + \mathbf{G}_i^{(Q)}(\tilde{b}))^2 \mathbf{X} \left[\alpha \mathbf{M}^{(0)} + \sum_{p=1}^P \tilde{b}^p \mathbf{M}_i^{(p)} \right]^{-1} \mathbf{x}'_i \\
&= \sum_i \mathbf{x}_i \left[\alpha \mathbf{M}^{(0)} + \sum_{p=1}^P \tilde{b}^p \mathbf{M}_i^{(p)} \right]^{-1} (\alpha^2 \mathbf{X}' \mathbf{X} + 2\alpha \mathbf{X}' \mathbf{G}_i^{(Q)}(\tilde{b}) \mathbf{X} \\
&\quad + \mathbf{X}' \mathbf{G}_i^{(Q)}(\tilde{b})^2 \mathbf{X}) \left[\alpha \mathbf{M}^{(0)} + \sum_{p=1}^P \tilde{b}^p \mathbf{M}_i^{(p)} \right]^{-1} \mathbf{x}'_i \\
&= \sum_i \mathbf{x}_i \left[\alpha \mathbf{M}^{(0)} + \sum_{p=1}^P \tilde{b}^p \mathbf{M}_i^{(p)} \right]^{-1} (\alpha^2 \mathbf{M}^{(0)} + 2\alpha \sum_{p=1}^P \tilde{b}^p \mathbf{M}_i^{(p)} \\
&\quad + \sum_{p=1}^P \tilde{b}^{2p} \mathbf{M}_i^{(2p)}) \left[\alpha \mathbf{M}^{(0)} + \sum_{p=1}^P \tilde{b}^p \mathbf{M}_i^{(p)} \right]^{-1} \mathbf{x}'_i.
\end{aligned} \tag{A4}$$

Although we also need to calculate $\mathbf{M}_i^{(2p)}$, which is a $K \times K$ matrix whose (k, k') -th element is $\sum_j g_{i,j}(b_0)^{8/2p} x_{j,k} x_{j,k'}$, the computational complexity is identical to that of $\mathbf{M}_i^{(p)}$. Thus, the calculation is still trivial.

Given N^* , the unbiased estimate of the residual variance yields

$$\hat{\sigma}^2 = \frac{1}{N^*} \sum_{k=1}^K \left(y_i - \sum_{k=1}^K x_{i,k} \hat{\beta}_{i,k} \right)^2. \tag{A5}$$

The variance estimates for the SVCs are derived as

$$\begin{aligned}
Var[\hat{\boldsymbol{\beta}}_i] &= \hat{\sigma}^2 (\mathbf{X}' \tilde{\mathbf{G}}_i(\tilde{b}, \alpha) \mathbf{X})^{-1} \mathbf{X}' \tilde{\mathbf{G}}_i(\tilde{b}, \alpha)^2 \mathbf{X} (\mathbf{X}' \tilde{\mathbf{G}}_i(\tilde{b}, \alpha) \mathbf{X})^{-1}, \\
&= \hat{\sigma}^2 \left[\alpha \mathbf{M}^{(0)} + \sum_{p=1}^P \tilde{b}^p \mathbf{M}_i^{(p)} \right]^{-1} (\alpha^2 \mathbf{M}^{(0)} + 2\alpha \sum_{p=1}^P \tilde{b}^p \mathbf{M}_i^{(p)} \\
&\quad + \sum_{p=1}^P \tilde{b}^{2p} \mathbf{M}_i^{(2p)}) \left[\alpha \mathbf{M}^{(0)} + \sum_{p=1}^P \tilde{b}^p \mathbf{M}_i^{(p)} \right]^{-1},
\end{aligned} \tag{A6}$$

which is again trivial to calculate. Thus, diagnostics of the ScaGWR are available for large samples.

Note that the CP time presented in Section 4 includes the time taken to estimate both $\hat{\beta}_i$ and $Var[\hat{\beta}_i]$.

By calculating $tr[\mathbf{S}]$, $tr[\mathbf{S}'\mathbf{S}]$, and $\hat{\sigma}^2$ in the way explained above, the corrected Akaike Information Criterion (AICc), which is formulated as follows, is calculated computationally efficiently:

$$AICc = N \log(\hat{\sigma}^2) + N \log(2\pi) + N \frac{N + tr[\mathbf{S}]}{N - 2 - tr[\mathbf{S}]} \quad (A7)$$

The LOOCV can be substituted with AICc-based bandwidth optimization by using Eq. (A7).

References

- Banerjee, S., Gelfand, A. E., Finley, A. O., and Sang, H. (2008) Gaussian predictive process models for large spatial data sets. *Journal of the Royal Statistical Society: Series B (Statistical Methodology)*, 70 (4), 825-848.
- Bishop, C. M. (2006) *Pattern Recognition and Machine Learning*. Springer, New York.
- Brunsdon, C., Fotheringham, S., and Charlton, M. (1998) Geographically Weighted Regression. *Journal of the Royal Statistical Society: Series D (The Statistician)*, 47 (3), 431-443.
- Cahill, M. and Mulligan, G. (2007) Using geographically weighted regression to explore local crime patterns. *Social Science Computer Review*, 25 (2), 174-193.
- Casetti, E. (1972) Generating models by the expansion method: applications to geographical research. *Geographical analysis*, 4 (1), 81-91.
- Cressie, N. (1993) *Statistics for Spatial Data*. John Wiley and Sons, New York.
- Cressie, N. and Johannesson, G. (2008) Fixed rank kriging for very large spatial data sets. *Journal of the Royal Statistical Society: Series B (Statistical Methodology)*, 70 (1), 209-226.
- Datta, A., Banerjee, S., Finley, A. O., and Gelfand, A. E. (2016) Hierarchical nearest-neighbor Gaussian process models for large geostatistical datasets. *Journal of the American Statistical Association*, 111 (514), 800-812.
- Dong, G., Nakaya, T., and Brunsdon, C. (2018) Geographically weighted regression models for ordinal categorical response variables: An application to geo-referenced life satisfaction data. *Computers, Environment and Urban Systems*, 70, 35-42.
- Dray, S., Legendre, P., and Peres-Neto, P. R. (2006) Spatial modelling: a comprehensive framework for principal coordinate analysis of neighbour matrices (PCNM). *Ecological Modelling*, 196 (3-4), 483-493.
- Eddelbuettel, D. 2013. *Seamless R and C++ Integration with Rcpp*. New York: Springer.
- Fan, J., Heckman, N. E., and Wand, M. P. (1995) Local polynomial kernel regression for generalized linear models and quasi-likelihood functions. *Journal of the American Statistical Association*

Association, 90 (429), 141-150.

- Finley, A. O. (2011) Comparing spatially - varying coefficients models for analysis of ecological data with non - stationary and anisotropic residual dependence. *Methods in Ecology and Evolution*, 2 (2), 143-154.
- Finley, A. O., Datta, A., Cook, B. C., Morton, D. C., Andersen, H. E., and Banerjee, S. (2018) Efficient algorithms for Bayesian nearest-neighbor Gaussian processes. *Journal of Computational and Graphical Statistics*, DOI: 10.1080/10618600.2018.1537924.
- Fotheringham, A. S., Brunson, C., and Charlton, M. (2002) *Geographically Weighted Regression: The Analysis of Spatially Varying Relationships*. Wiley, New York.
- Fotheringham, A. S., Yang, W., and Kang, W. (2017) Multiscale geographically weighted regression (mgwr). *Annals of the American Association of Geographers*, 107 (6), 1247-1265.
- Geniaux, G. and Martinetti, D. (2018) A new method for dealing simultaneously with spatial autocorrelation and spatial heterogeneity in regression models. *Regional Science and Urban Economics*, 72, 74-85.
- Gollini, I., B. Lu, M. Charlton, C. Brunson & P. Harris (2015) GWmodel: an R Package for Exploring Spatial Heterogeneity using Geographically Weighted Models. *Journal of Statistical Software*, 63, 1-50.
- Harris, R., Singleton, A., Grose, D., Brunson, C., and Longley, P. (2010) Grid - enabling geographically weighted regression: a case study of participation in higher education in England. *Transactions in GIS*, 14 (1), 43-61.
- Harris, P. (2019) A simulation study on specifying a regression model for spatial data: Choosing between autocorrelation and heterogeneity effects. *Geographical Analysis*, 51 (2), 151-181.
- Heaton, M. J., Datta, A., Finley, A. O., Furrer, R., Guinness, J., Guhaniyogi, R., Gerber, F., Gramacy R. B., Hammerling, D., Katzfuss, M., Lindgren, F., Nychka, D. W., Sun, F., and Zammit-Mangion, A. (2018) A case study competition among methods for analyzing large spatial data. *Journal of Agricultural, Biological and Environmental Statistics*, DOI: 10.1007/s13253-018-00348-w.
- Leong, Y.-Y. & J. C. Yue (2017) A modification to geographically weighted regression. *International Journal of Health Geographics*, 16, 11.
- Li, Z., Fotheringham, A. S., Li, W., and Oshan, T. (2019) Fast Geographically Weighted Regression (FastGWR): a scalable algorithm to investigate spatial process heterogeneity in millions of observations. *International Journal of Geographical Information Science*, 33 (1), 155-175.
- Liu, H., Ong, Y. S., Shen, X., and Cai, J. (2018) When Gaussian process meets big data: A review of scalable GPs. *ArXiv*, 1807.01065.
- Lu, B., Charlton, M., Harris, P., and Fotheringham, A. S. (2014a). Geographically weighted

regression with a non-Euclidean distance metric: a case study using hedonic house price data. *International Journal of Geographical Information Science*, 28 (4), 660-681.

- Lu, B., P. Harris, M. Charlton & C. Brunsdon (2014b) The GWmodel R package: further topics for exploring spatial heterogeneity using geographically weighted models. *Geo-spatial Information Science*, 17, 85-101.
- Lu, B., M. Charlton, C. Brunsdon & P. Harris (2016) The Minkowski approach for choosing the distance metric in Geographically Weighted Regression. *International Journal of Geographical Information Science*, 30, 351-368.
- Lu, B., Brunsdon, C., Charlton, M., and Harris, P. (2017) Geographically weighted regression with parameter-specific distance metrics. *International Journal of Geographical Information Science*, 31 (5), 982-998.
- Lu, B., Yang, W., Ge, Y., and Harris, P. (2018) Improvements to the calibration of a geographically weighted regression with parameter-specific distance metrics and bandwidths. *Computers, Environment and Urban Systems*, 71, 41-57.
- Lu, B., C. Brunsdon, M. Charlton & P. Harris (2019) A response to 'A comment on geographically weighted regression with parameter-specific distance metrics'. *International Journal of Geographical Information Science*, 1-13.
- Mu, J., Wang, G., and Wang, L. (2018) Estimation and inference in spatially varying coefficient models. *Environmetrics*, 29 (1), e2485.
- Murakami, D., and Griffith, D. A. (2019) Spatially varying coefficient modeling for large datasets: Eliminating N from spatial regressions. *Spatial Statistics*, 30, 39-64.
- Murakami, D., Lu, B., Harris, P., Brunsdon, C., Charlton, M., Nakaya, T., and Griffith, D. A. (2019) The importance of scale in spatially varying coefficient modeling. *Annals of the American Association of Geographers*, 109, 1-21.
- Murakami, D., Yoshida, T., Seya, H., Griffith, D. A., and Yamagata, Y. (2017) A Moran coefficient-based mixed effects approach to investigate spatially varying relationships. *Spatial Statistics*, 19, 68-89.
- Nakaya, T., Fotheringham, A. S., Brunsdon, C., and Charlton, M. (2005) Geographically weighted Poisson regression for disease association mapping. *Statistics in Medicine*, 24 (17), 2695-2717.
- Oshan, T., L. J. Wolf, A. S. Fotheringham, W. Kang, Z. Li & H. Yu (2019) A comment on geographically weighted regression with parameter-specific distance metrics. *International Journal of Geographical Information Science*, 1-12.
- Páez, A., Long, F., and Farber, S. (2008) Moving window approaches for hedonic price estimation: an empirical comparison of modelling techniques. *Urban Studies*, 45 (8), 1565-1581.
- Rue, H., Martino, S., and Chopin, N. (2009) Approximate Bayesian inference for latent

Gaussian models by using integrated nested Laplace approximations. *Journal of the royal statistical society: Series b (statistical methodology)*, 71 (2), 319-392.

- Stein, M. L. (2014). Limitations on low rank approximations for covariance matrices of spatial data. *Spatial Statistics*, 8, 1-19.
- Tran, H. T., Nguyen, H. T., and Tran, V. T. (2016) Large-scale geographically weighted regression on Spark. *Proceedings of the 2016 Eighth International Conference on Knowledge and Systems Engineering*, pp. 127-132. IEEE.
- Tsutsumida, N., Rodríguez-Veiga, P., Harris, P., Balzter, H., and Comber, A. (2019) Investigating spatial error structures in continuous raster data. *International Journal of Applied Earth Observation and Geoinformation*, 74, 259-268.
- Wheeler, D. and Tiefelsdorf, M. (2005) Multicollinearity and correlation among local regression coefficients in geographically weighted regression. *Journal of Geographical Systems*, 7 (2), 161-187.
- Wolf, L. J., Oshan, T. M., and Fotheringham, A. S. (2018) Single and multiscale models of process spatial heterogeneity. *Geographical Analysis*, 50 (3), 223-246.
- Yang, W. (2014) An extension of geographically weighted regression with flexible bandwidths. *Doctoral dissertation*, University of St Andrews.